Planar Antennas for Wireless Power Transfer at mmWaves

Francisco Filipe Silva Lopes da Ressurreição Martins
francisco.ressurreicao@tecnico.ulisboa.pt

Instituto Superior Técnico, Universidade de Lisboa, Lisboa, Portugal

***Abstract*—With the demand for better, smaller and cheapest satellites to use for space mission purposes, Cubesats, satellites of small dimensions that allow to be launched in a higher quantity with low production costs, are establishing as one of the most prolific satellites to consider. More specifically, with cubesats of 1U and 3U dimensions, it is possible to execute missions with cubesats constellations, that make the results achievement quicker and easier. For missions using cubesats constellations, the storing and transfer of energy from one satellite to another may be a key strategy to guarantee the best performance possible. The purpose of this thesis is to study the impact on the power transfer efficiency of using Gaussian beams to wirelessly transfer energy from a cubesat to another. Specifically, taking a 3U cubesat, wirelessly transferring power to a smaller cubesat, 1U, at distances within the near-field range. To do so, a system of two opposite reflectarrays antennas (RA), are designed and fabricated to generate the Gaussian beam and focus its energy into a collecting aperture. The used RAs are low-cost planar structures, fabricated with printed circuit technology, populated with 2-square rings unit cells, to achieve the required phase front correction, at 24 GHz. Each RA uses a horn antenna at its focus, one to illuminate the larger RA with energy, and the other to receive the energy collected by the smaller RA. This strategy, together with the use of the Gaussian beam ensure a significant reduction of wasted energy by "spill-over", compared to simple wave propagation between two antennas.**

***Keywords*: satellites, CubeSats, wirelessly transfer power, antennas, reflectarrays, ka band, phoenix cells, directivity..**

I. Introduction

For a lot of satellites missions, one of the biggest issues is the durability of their energy. It is not endless, nor can be continuously restored throughout the mission. One of the possible solutions is to implement on the satellites solar panels that can absorb sun energy and turn it into electrical energy, capable to sustain the functionalities of the satellite. But with this comes another issue: the size of the satellites. For bigger satellites this can be a main solution, but for smaller satellites, like the CubeSats, it doesn't solve the problem since, due to their size, they can't support big solar panels, which means they can't absorb enough quantity of solar light to restore their energy. They must have deployable panels, so it doesn't affect their performance nor their launch to space. One thing that can represent a solution for this problem is the fact that, for most of the situations, these small satellites operate in "constellations", meaning they are launched into space in a certain number and work as a team, covering a much larger area. If there are different sizes of satellites, it may be viable to use some of them, of bigger size, to receive the Sun energy and share it with other smaller satellites, through antennas manufactured specifically for that purpose. This solution must be, obviously, wireless, and it needs to be able to operate for short distances, since the satellites won't be too much far from each other. On the other hand, the way the power is transmitted must be such that it avoids at the maximum the amount of energy that is wasted by "spill-over". The result is a fully working constellation of small satellites that can cover a considerable area of space, that can fulfil their missions, from gathering space particles for study, studying the weather or even for telecommunication purposes. So the main goal of this work is to study if reflectarray antennas, configured to produce Gaussian beams, will wirelessly transfer power, from one Cubesat to another, focusing the maximum intensity possible on the desired collecting surface area, with the best energy transfer efficiency possible. Reflect-arrays are planar, foldable to compact volume, and have low mass; therefore, they are a natural choice for use in smallsats. In fact, due to the CubeSats sizes, the antennas are limited in area and mass: while for the 1U CubeSat, the smallest one, the RA can have a maximum area of 10x10 cm, in the case of the 3U the area will be 30x30 cm, and it has to be folded for launch. This RA's area difference has also an impact on the process of studying and fabricating each RA prototype. Since the cubesats are nanosattelites, with a mass between 1 kg to 10 kg, the RAs must be flat, not only to reduce the total area of the cubesat but to avoid increasing as much as possible its maximum mass. Furthermore, the distance between the two satellites also has an impact, since it affects the intensity the beam leaves one reflectarray and focuses on the other one. The appropriate operation frequency for WPT must be chosen as a compromise between the size of the transmitting, and collecting antenna surfaces, the focusing distance, and the RF-DC conversion efficiency. The 24 GHz frequency was established as this compromise. In the end, and after considering all the conditions and restrictions mentioned above, the desired efficiency is the main goal to be kept in mind: for a ratio DRx/w0 close to one, being DRx the size of the transmitting reflect-array and w0 the minimum waist of the Gaussian beam, the transfer efficiency should achieve relatively high values, over 80%Ḣowever, the system has inherent losses, associated with energy spillover past the edges of the reflect-arrays and respective feeds, and reflection

efficiency of the reflect-array unit cells. The objective of this thesis, is to fully characterize the proposed WPT system by simulation and the experimental prototype.

II. Small Satellites - CubeSats Harvesting

During the XX century, and with the Cold War's Space Run ongoing, the appearance of available microelectronic components enabled the construction of smaller and smaller satellites, with smaller teams, since each space mission, concerning the building of the satellite and required advanced and expensive technologies, was a costly, risky and complex program [1]. The two small satellites conferences held in 1987 culminated in January 21, 1990 with the launch of the French SPOT-2 Earth resources satellite by an Ariane-4, along with 5 microsatellites. This was the first flight of the Ariane Structure for Auxiliary Payload (ASAP) ring, able to hold up six small satellites (50-kg mass maximum) with 35 x 35 x 60 cm dimensions maximum. Those AMSAT microsatellites, that can be considered nanosatellites with today's satellites standards, were 23-cm dimension cubes covered with solar cells (maximum output power of 15.7 W).

More and more picosatellites and nanosatellites were placed in orbit throughout the years and in June 2000 an important nanosatellite milestone was achieved, when the 6.5-kg mass SNAP-1 was launched along with the 50-kg mass Tsinghua-1 microsatellite, this last one with the purpose of serving as a target platform for a satellite inspection mission [2]. This successful mission led Stanford and the California Polytechnic State University at San Luis Obispo to create and establish a whole new program dedicated to CubeSat [2].

A. Reflect Arrays

Regarding the frequency range used on this project (between 20-30 GHz), antennas that operate on this level are much more compact and have higher gain and much lower cost. When choosing the type of high gain antenna capable of beam steering for a specific project, normally aperture antennas or antenna arrays are the ones considered. Usually aperture antennas are bulkier when compared to antenna arrays, which requires the integration on the mechanic of the craft, highly increasing its weight, cost and time of implementation and launch cost. In that way, a much lighter and non expensive solution are the antenna arrays [7]. This sub chapter focuses on different types of those antennas, to provide knowledge about the technology used for this project.

One of the approaches to realize a high gain is based on antenna array theory where interference of elements radiation is controlled. A transmit array (TA) antenna is described as a set of a flat transmitting surface illuminated by a feed source, located on a focal point. The flat surface is composed of one or multiple layers, where there is a printed antenna elements array. The basic function of these elements, regarding their transmission coefficients, is to transform from a spherical phase front to a planar phase front, resulting in a high gain radiation beam [3].

The array consists of many small antennas that are responsible for the phase shift and make possible to achieve a high gain. For that reason, they are typically used for high frequency end of the radio spectrum, in microwave bands, in which the antenna elements are small [4].

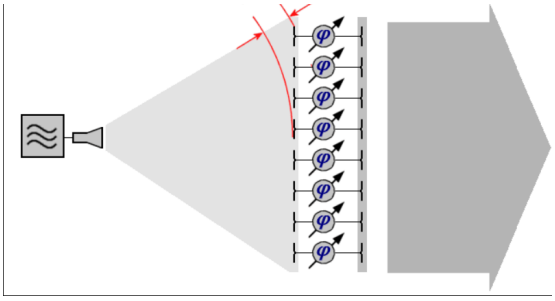

Fig. 1: Reflect Array and phase shift process.

A reflect array (RA) have similar functionality when compared to a transmit array. It is the combination of reflector antennas and phased array antennas working principles. It has a feed, also located at a focal point, and a planar surface where are located the unit cells responsible for the phase shift. After the phase shift happens, instead of being transmitted as a steering beam, the planar metallic surface will reflect the beam with an angle that depends on the incident angle of the wave.

B. Unit Cells

Like dielectric lens working principle, in every zone of the RA or the TA, an appropriate phase shift is added to the incident field. This phase shift is provided by individual constant thickness unit cells, that are distributed along the whole planar surface of the TA/RA. This gives a big advantage comparing to lenses, where the phase shift is provided by adjusting its profile, since it requires much less mass and offers more flexibility.

Despite having constant thickness and the same size, unit cells are designed to present different phase shift values throughout the planar surface. This unit cells must ensure minimum reflection and insertion loss, as well as a phase range that goes up to 360 degrees to ensure every point of the surface has a phase correction of the incident wave so it can produce continuous phase radiation results [5]. Even considering a certain number of levels in the [0, 360] degrees range, enough to obtain those radiation results, and unit cells are designed for infinite periodic surfaces, the reality is that adjacent cells are not equal, the size changes according to the phase distribution. This means that the larger the phase transition between adjacent cells, the larger the phase and reflection loss degradation [6].

III. Wireless Power Transfer

With a lot of new possibilities for new ways to store and use energy, one that stoods out was the Wireless Power Transmission/Transfer (WPT). Since there's unlimited Solar

energy supply in space, free from weather conditions, it seems that finding an alternative for fossil fuels, taking advantage of the sun, is probably one of the most plausible ways to do it [8]. The concept, conceived by Dr. Peter Glaser in 1973, was to harvest large amounts of solar energy (with satellites in geostationary Earth Orbit (GEO)), transform it in microwave energy and then transmit it to a rectifying antenna (rectenna) array on Earth that would collect and convert the energy into usable direct current power. It is expected that one day this system could supply enough electrical power to Earth and ensure to humanity the continuation of advancement. WPT has been an active topic of research, and, since then, many WPT schemes have been implemented in near-field (coupling) and far-field (radiation) regimes. As mentioned before, it can deliver power without wiring infrastructures.

However, the big challenge has been to achieve high efficiency systems at reasonable transfer distances. Although these systems are safe in terms of exposure for humans, and even though they are highly efficient at short distances, the usual WPT schemes require the receiving device to be near the power source. On the other hand, power transfer can be accomplished using short wavelength radio frequency (RF) power radiated from a source aperture to a receive antenna/aperture [10], [11].

Usually, space missions operate either from an onboard nuclear power source or using onboard solar power generation panels. In both ways, the available power and its utilization rate are limited, which can be a handicap for longer time missions [9]. A new approach, using space solar power (SSP) satellites to provide power to other spacecrafts, taking advantage of the unlimited solar energy source started to emerge [9]. When transferring this system to be conceded for space missions, there are some factors to consider, since the idea is to transfer energy from one satellite to another. This implies the consideration of the working frequency, compromised between antenna size and atmospheric attenuation, the material used to build the spacecraft, beam pointing energy to transmit the microwave power beam precisely to the receiving site and power efficiency, among others [8].

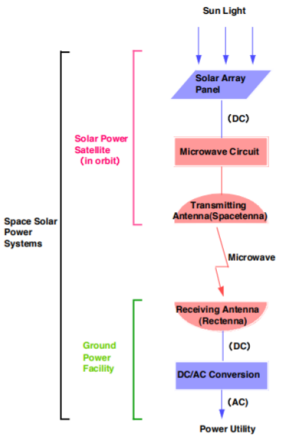

Fig. 2: Space Solar Power Systems.

IV. Basic concepts and physical principles

A. Gaussian Beam

A Gaussian Beam can be described as a beam, usually a laser beam, which electrical field profile in a plane perpendicular to the beam axis is given by a Gaussian function. The evolution, through space, of the beam's intensity, is described as

$$\mathbf{I}(r,z) = \frac{P}{\pi w(z)^2/2} e^{\frac{-2r^2}{w(z)^2}} \tag{1}$$

where r is the radial distance away from the axis, w(z) is the radius of the laser beam where the irradiance is 1/e2 (13.5%) of the maximum value, z is the distance propagated from the plane where the wavefront is flat and P is the total power of the beam.

The fact that in the centre of the beam the intensity is at its highest, does not mean that it will remain always with approximately the same values. Due to diffraction, the Gaussian beam converges and diverges from what is called the minimum beam waist w0, where the beam diameter reaches its minimum. Assuming that the electric field is focused from the aperture of diameter D and focal length z0 the minimum beam waist can be calculated as

$$\mathbf{w}_0 = \frac{4}{\pi} \frac{z_0 \lambda}{D cos(\theta)^2} \tag{2}$$

Where is the angle between the optical axis of the aperture and the vector defined from the aperture centre to the position of the focus.

As said before, due to diffraction phenomenon, the beam waist will not remain constant as it varies along the propagation direction. It can be mathematically described as

$$\mathbf{w}(z) = w_0 \sqrt{1 + (\frac{z}{z_R})^2} \tag{3}$$

With the Rayleigh length,

$$\mathbf{Z}_R = \frac{\pi w_0^2}{\lambda} \tag{4}$$

Which determines the length over which the beam can propagate without diverging significantly.

By analysing the equation (5), at the position $z = 0$, the beam waist will have its minimum value, the focus of the beam, and the phase profile is flat [13].

B. Phase Shift

Through a feed, located at a focal point O, a spherical wave is transmitted and will focus on a surface S, where the lens of the reflect array is located, and that will receive the fields of that incident wave.

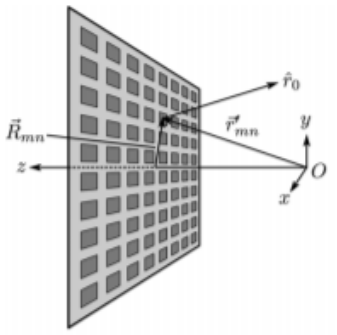

Fig. 3: Incident wave on the RA.

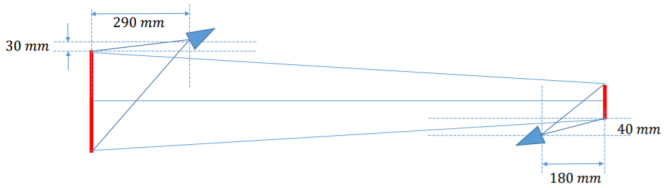

Fig. 4: Full geometry of the problem.

Since it is a spherical wave, as mentioned before, once it focuses the lens, due to its curvature, it will not focus on every point with the same phase, besides the fact that the rays originated from the feed do not have all the same direction when illuminating the lens. The result is a lens with points with different phases, when the goal is to reflect a plane wave, with the same phase in all its points.

The total phase is originated according to two important factors: the phase of the incident electric field on the lens and the phase shift added by the lens itself when the wave is reflected.

In Cartesian coordinates, the following equation,

$$\mathbf{r}_{mn} = \sqrt{(x - x_{feed})^2 + (y - y_{feed})^2 + (z - z_{feed})^2} \quad (5)$$

represents the distance between the feed and a point on the aperture.

Since the main goal is to reflect the plane wave to a specific point, we can define it for a first focus, which will be the lens itself, and a second one, at a positioned previousily defined.

Therefore, the distance from the feed to the focal point, including the reflection performed by the lens, is defined as

$$\mathbf{r}_{total} = r_1 + r_2 \quad (6)$$

applying the positions of the first focus, $(x_{focus1}, y_{focus1}, z_{focus1})$, and the second one $(x_{focus2}, y_{focus2}, z_{focus2})$ to the equation (6), where there is the coordianted position of the feed.

It is now possible to define the electric field phase distributions, phi, when the wave focuses on the lens and when it is reflected [6].

$$\phi_1 = \sqrt{(x - x_{focus1})^2 + (y - y_{focus1})^2 + (z - z_{focus1})^2} \quad (7)$$

$$\phi_2 = \sqrt{(x - x_{focus2})^2 + (y - y_{focus2})^2 + (z - z_{focus2})^2} \quad (8)$$

Having defined the electric field phase distributions, which must be negative as they represent the distancing of the wave from the feed, it is now vital to add the phase shift added by the RA itself. The phase correction expression results from applying the condition

$$\phi_1 + \phi_2 + \phi_{lens} = constant \quad (9)$$

Which leads to

$$\phi_{lens} = -\phi_1 - \phi_2 + constant \quad (10)$$

In the case of the 10 cm x 10 cm RA, the expression does not need to take into consideration the focusing distance of the beam. The beam can be considered a collimated one, reducing its expression to

$$\phi_{10lens} = k_0(-\sqrt{(x - b)^2 + y^2 + (z - F_{in10})^2} + xsin(\alpha_0)) \quad (11)$$

Furthermore, when checking the phase on each point of the lens, since the phase range goes from 0 to 360 degrees, there can be some adjacent points where there are phase jumps of 360 degrees. These jumps are called zoning cases and must be prevented. Defining as the distance between a point on the aperture and the projection of the feed on the plan xy (z = 0).

$$\rho = \sqrt{(x - x_{feed})^2 + (y - y_{feed})^2} \quad (12)$$

It is possible to ensure that for a ρ smaller than a defined jump ray, the lens will be in zoning, otherwise that situation will not be considered.

V. Formulation and methods

A. Overall geometry

For the wireless power transfer between the two satellites, the geometry used had to take into account the size of the RAs, the position of the feeds (and their distance to the RAs), the distance between both satellites and also the beam waist. Therefore, to guarantee that this study could be completed, it was decided to proceed with the following geometry:

From the bigger satellite, on the left side of the figure, the feed will radiate the beam to the RA surface to then be transmitted. Once it is transmitted, it will travel a certain distance, approximately 1.5 meters, until it gets to the second RA, attached to the smallest satellite. After this, the process is similar, though in the reverse direction, since this time the RA will reflect the light beam back to the second feed, positioned near it. The first feed will be positioned 180 mm of the centre of the lens and at a height of 290 mm, while the second feed

will be 90 mm distanced from the lens centre and at a height of 180 mm.

B. Reflected and incident angles

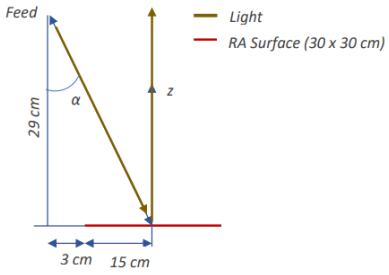

Fig. 5: First feed angle.

The first feed, corresponding to the one near the biggest RA (Figure 3) will radiate the beam light focusing the RA with a specific angle. This angle, α, is dependent on the position of the feed regarding the position of the RA. Using the Pythagoras Theorem, it is possible to determine the angle, taking into consideration the distances from Figure 5:

$$\alpha = \arctan(\frac{18}{29}) = 31.83° \tag{13}$$

From Figure 4, the light beam reflected by the biggest RA will be radiated linearly with its geometry, meaning, the reflected angle will be zero and the light beam direction will be perpendicular to the RA surface. For this reason, feeds must not be on the line of sight of the beam direction, from one satellite to another. Therefore, the feeds position where decided and presented as in Figure 3.

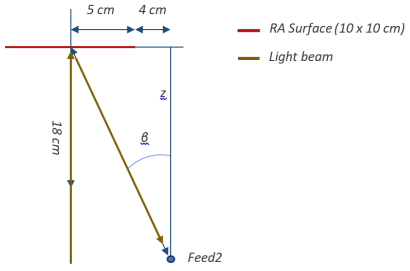

Fig. 6: Second feed angle.

Now for the second feed and the beam reflected by the smallest RA, the reflected angle also depends on the position of the feed. In this case, the reflected angle, by simple calculations, is:

$$\beta = \arctan(\frac{9}{18}) = 26.57° \tag{14}$$

The distance between the two satellites, meaning, the distance the beam reflected by the biggest RA will travel until it gets to the smallest RA, is 1.5 m. This distance defines the region where the satellites will work as the near field, where the waves and their nature are dependent on the distance to the antenna. This will make the difference between being possible to focus a Gaussian beam or having collimated rays (the rays leaving the edges of the RA's surface are parallel).

VI. Design and simulation results

To obtain the Gaussian beam, it is necessary to define the phase shifts of the lenses and, more specifically, of the unit cells. This also affects the direction of the reflected beam, so it is mandatory to define the phase laws related to each antenna. Since both lenses are filled with unit cells, responsible for the phase correction, it is important to define the desired phase for each cell, to reflect the beam with both desired direction and phase. To present a full structured study over all the aspects of the geometry, as well as to better understand the inputs and outputs of the whole system, from one satellite to another, the process was divided in two problems: the beam being transmitted by the first feed and being reflected by the first RA; and the second problem where the already reflected beam hits the second RA, being then reflected towards the second feed.

(a) Geometry of the first problem.

(b) Geometry of the second problem.

Fig. 7: Problem's geometry divided into two parts.

A. Transmit Array examples

The whole process' behaviour is simulated with the use of a Mathematica notebook. Transmit arrays are used, since they work with the same phase shift method way as reflect arrays. For the simulations matter, both TAs and feeds are defined for specific positions and sizes to implement the idea of the phase shift. The objective is to simulate a planar RA to produce a Gaussian beam. The two RAs widths are of 30 cm for the largest RA, and 10 cm for the small one. The study is performed at 24 GHz Another factor to take into consideration is the conversion efficiency from radio frequency to DC (direct current), since it drops with the increase of the frequency. Taking all these factors into consideration, a reasonable frequency value would be between 20-30 GHz. For this reason, the 24 GHz frequency was chosen to proceed with the study.

Considering the focus distances of the feeds to the apertures, the result is a beam focused near the centre of the RA, since the angle of the feed makes the beam focus with different phase

along the RA, both in magnitude and phase. This was a crucial step to define the phase laws for each unit cell implemented on the RA, from their phase difference from the centre.

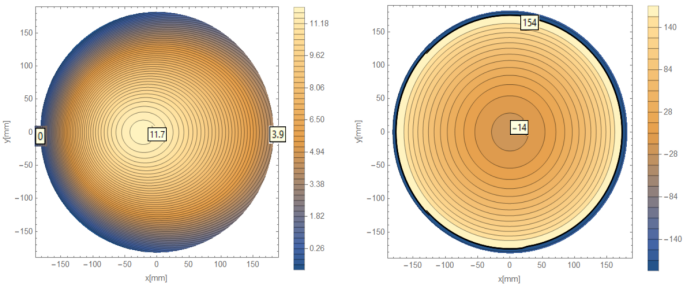

Fig. 8: beam focus on the 30x30 cm lens: left side directivity in dB on the lens; right side phase distribution of the beam on the lens.

For the magnitude, the tapper between the centre and the edge of the lens is approximately 10 dB, the value established in the begging of this work as the target value to achieve. It is also possible to infer, from the right side of Figure 5, that the wave does not hit the lens with the same phase in every point, proving the need to add a phase shift on the surface to allow to reflect a planar front wave. After the phase correction provided by the lens, the beam wave focuses at 1.5 m, meaning it has its lowest beam waist at this point and, consequently, maximum directivity. The phase is planar, confirming the phase shift of the initial spherical wave.

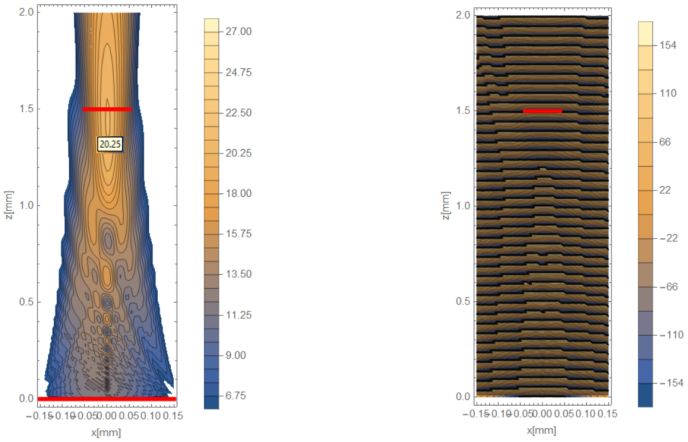

Fig. 9: Beam wave reflected by the biggest RA and focusing on the second RA: Gaussian Beam directivity across the 1.5m distance (left side); Gaussian Beam planar front wave phase across the 1.5m distance (right side).

The beam that leaves the second lens is already a spherical wave, which means that, after the phase correction, the beam phase presents an angled beam direction, to hit the second feed position, and a phase distribution that, different from before, is as it shows in Figure 7.

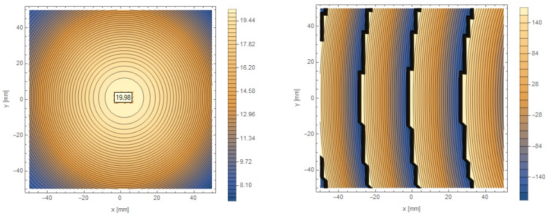

(a) Second lens magnitude and phase after the phase shift. (XY plane)

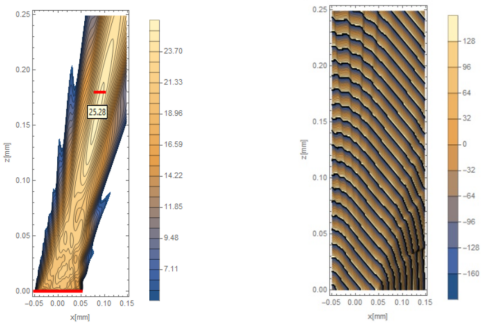

(b) Phi=0 plane for the far field simulation.

Fig. 10: Gaussian Beam that exits the lens and focuses on the feed (left side - magnitude, right side - phase) [XZ plane].

B. Unit Cells design and simulation

The design of the unit cells is composed of a PEC base (a metal material), a substrate material and finally two copper rings, one outer and one inner, that will be modified for the phase range needed.

Since each unit cell as dimensions of 3 cm over 3 cm, both substrate and metal, it needed to check those same dimensions. Also, both have the same thickness (z axis), of 0.787 cm, with the substrate, called Rogers RT5880 (lossy), having a 2.2 permittivity. The square rings are made of copper (pure). This means that they have an electric conductivity of 5.96e +07 [S/m]. For the simulations, the three parameters of the unit cell's rings vary to successfully achieve a 0 to 360 degrees range, a full coverage of the entire phase spectrum to be able to correctly shift the phase. As shown in Figure 8, r01 represents the dimension of the outer ring's size, rg is the gap between both rings and rw is the thickness of both rings.

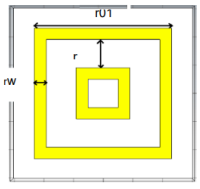

Fig. 11: different dimensions of the unit cell to be tested.

The simulations were performed on CST MicroWave Studio. The scattering parameter usually describes the power transfer between two ports. For instance, since we are dealing with an antenna, a common one-port network, it will be a 1x1

matrix, meaning that S11 will indicate the amount of radiated or dissipated power by the antenna. More specifically, it is necessary to verify both magnitude and phase of the S11: magnitude (dB) since it is important to have results has near to zero as possible (and no higher than -0.5 dB), and phase because the objective, as mentioned before, is to have a full 0 to 360 degrees range, with phase jumps no higher than 60 degrees. The rg and the rw parameters varied from 0.1 to 0.5 cm, while r01 varied from 0.2 up to 2.9 cm, to obtain all the possible unit cells designs for the phase range.

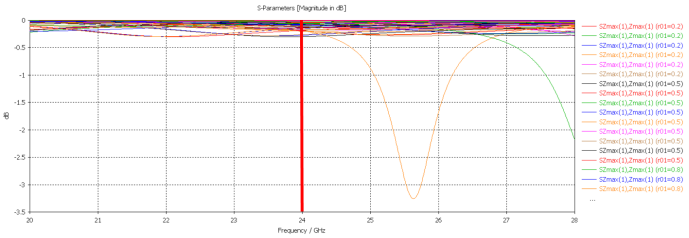

Fig. 12: S11 magnitude simulated for the unit cells parameters variation at 24 GHz

From Figure 9, at 24 GHz the magnitude of the S11 parameter clearly varies from 0 to -0.5 dB, which means that the majority of the light is reflected on the unit cell, having low energy losses. Without this magnitude results, it would be irrelevant to have a full phase range coverage, since the unit cells tested wouldn't be accurate enough. Now, for the phase testing, at 24 GHz, as mentioned before, it is mandatory to have no more than 60 degrees jumps.

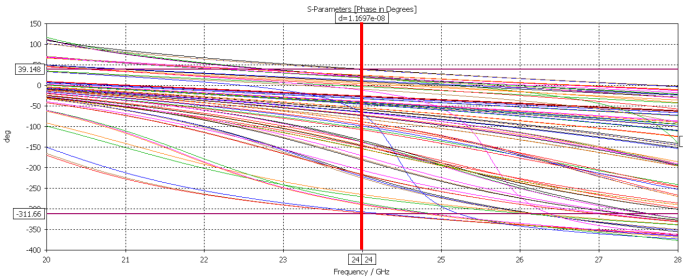

Fig. 13: S11 phase simulated for the unit cells parameters variation at 24 GHz

As shown in Figure 10, at 24 GHz, the different phase jumps, as a consequence of the variation of the S11 parameter, cover a degree spectrum from 39.148 to -311.66 degrees, completing the 360 degrees range necessary to completely cover the arriving wave that hits the lens with different phases across the surface. Since the maximum degree jumps accepted to have a validated simulation were stipulated at no higher than 60 degrees, even though there are areas where the phase jumps leave bigger gaps than in other areas, overall, it can be concluded that the degrees' simulation results were satisfactory to validate the unit cells.

C. Horn Simulation

The horn to be used in laboratorial experiences is vertical, tilted on the desired angle, without any type of bending on the structure itself. However due to software limitations, for the CST MWS software, the waveguide must be aligned with one of the coordinate planes, meaning it must be parallel with one of the symmetry planes

To overcome the waveguide plane issue, the waveguide is fixed and parallel to one of the symmetry planes, and to tilt the rest of the horn to have the best-approximated results. Since the aperture guides the direction of what comes from the horn, the waveguide was tilt with the necessary angle to reflect on the lens.

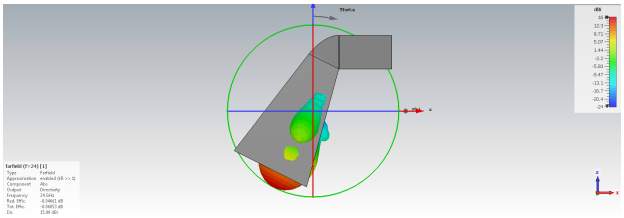

Fig. 14: Adapted Horn antenna with tilted waveguide

Has seen in Figure 11, the horn's curvature is placed at the connection between the aperture and the waveguide, to minimize the potential impact that the increase in size and deformation of the horn may have on the simulations. The simulation proved to be acceptable to proceed with the study, since the horn, even having a curvature and thus slightly changing its dimensions, maintains the same maximum directivity at the same frequency.

D. Lens Simulation

After all the calculations of the lens size, unit cells allocation and creation of the macro code, the study proceeds to the CST where the ".bas" file runs. The software first creates the metallic surface, on which each unit cell formed by the substrate material plus the copper rings is generated. After the conclusion of the generation of the lens, it is time to allocate the horn antenna to its geometric position and proceed with the parametric changes that allow a smoother and clearer simulation.

1) 10 cm Reflect Array

The 10 cm RA lens was simulated using the time domain solver of CST-MWS, resulting on the following far-field result:

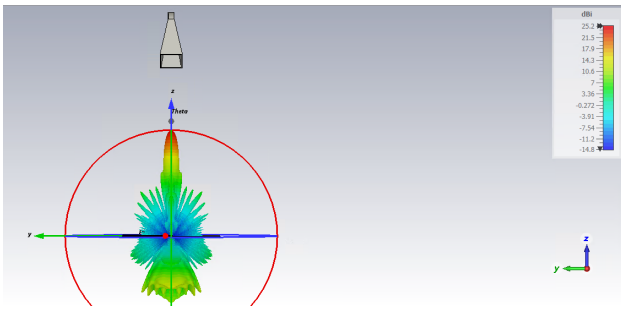

Fig. 15: far field results from a XZ plane perspective

While on the phi = 90 plane it is noticeable a perfectly symmetric radiation pattern, with the main lobe centred at theta = 0, on the phi = 0 plane, due to a shift of 1 degree in theta (the main lobe is centred at theta = 1), a not so symmetric radiation pattern is presented. Although the 1-degree shift may have influenced the simulation's symmetry, it doesn't critically affect the performance of the antennas due to the small distances they're projected to work on. Furthermore, by analysing the radiation waves on the different coordinate-plane views, it is noticeable that, after the phase shift produced by the lens, a plane wave is reflected perpendicularly to it, meaning, in the z direction

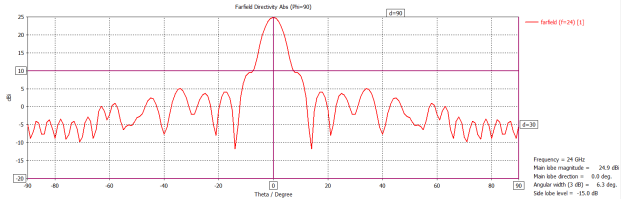

(a) Phi=90 plane for the far field simulation.

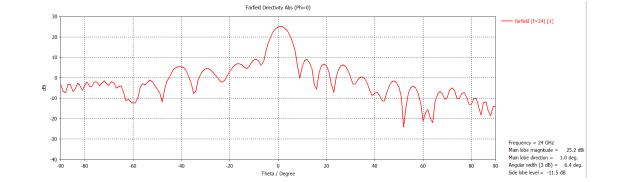

(b) Phi=0 plane for the far field simulation.

Fig. 16: RA's phi far field simulation in the phi=0 and phi=90 planes.

2) 30 cm Reflect Array

The study proceeds with the creation and simulation of the 30 cm RA. Due to its size the creation of this RA makes the CST file extremely heavy, which becomes a major problem for the simulation matter.

The same process is used to obtain the KH3D radiation pattern: a feed positioned at the desired point, radiating towards the 30 cm RA antenna, which then radiates it to the desired direction.

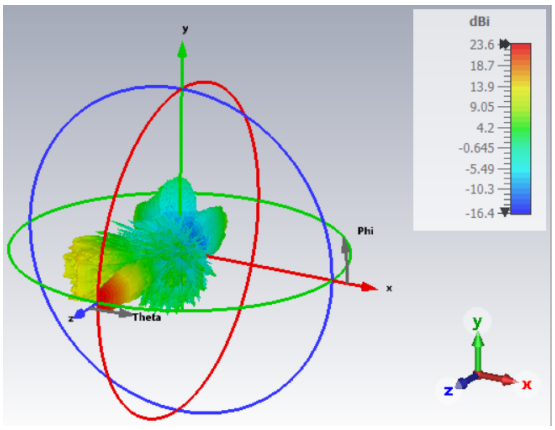

Fig. 17: farfield results for the 30 cm x 30 cm RA at 24 GHz.

On a first analysis, the radiation pattern presents an unexpected loss of about 14 dBi, closed to the focusing direction

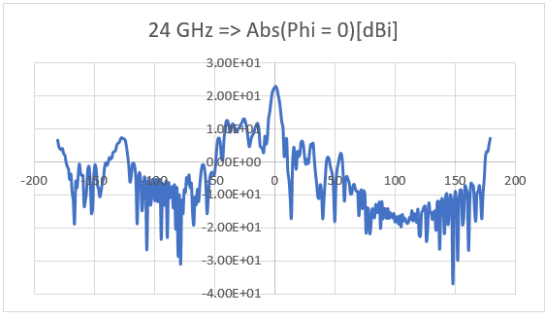

(a) Radiation pattern on the Phi = 0 plane.

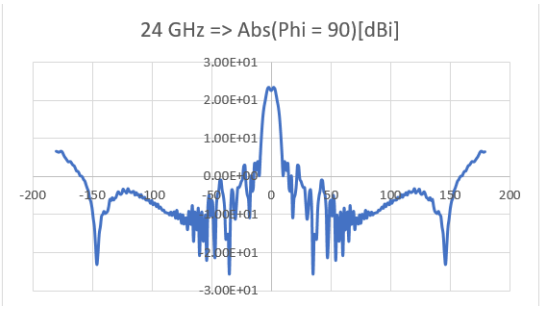

(b) Radiation pattern on the Phi = 90 plane.

Fig. 18: RA's phi far field simulation in the phi=0 and phi=90 planes.

For frequencies higher than 24 GHz, the radiation pattern tends to be better defined, and with higher gain. This may affect, in the future, the final efficiency of the system.

VII. Experimental Results

The following and final step of the simulations process is to perform experiments, first with the reflectarrays individually, then with the whole system of the RA combined. These experiments are performed in the anechoic chamber at Instituto Superior Técnico.

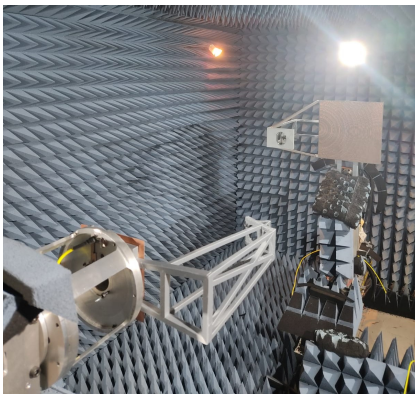

Fig. 19: Anechoic Chamber at Instituto Superior Técnico)

A. 10 cm Reflectarray

For the analysis of the following results, it is crucial to analyse the co-polarization graphic, which defines the desired polarization and direction, alongside with the signal strength

With the obtained results for the horn antenna it is possible to define the experimental gain and ,therefore, make a crucial comparison with the CST results. When comparing the co-polarization simulation with the results from the CST, not only the lobes (main and side) present a similar behaviour, but the difference between both gains is minimal.

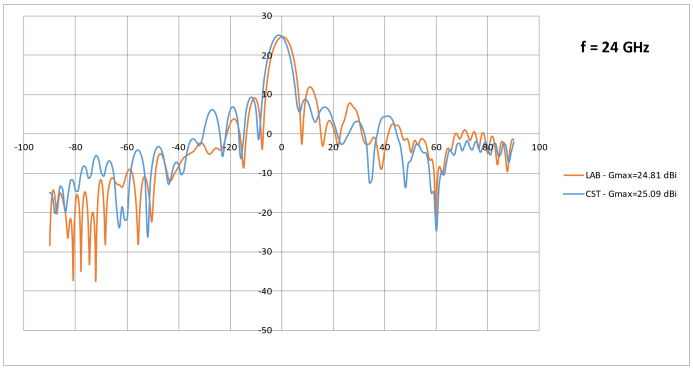

Fig. 20: Comparison between CST and experimental results at 24 GHz, with maximum gain information)

B. 30 cm Reflectarray

After the first RA's results are obtained and analysed, the same process runs through the 30 cm RA. Due to its large file size, it was not possible to simulate the polarizations, nor to obtain the gain. Therefore, the study made for this reflectarray is only based on the experimental results. The behaviour of the 30 cm RA shows a slight deviation in frequency, where at 24 GHz is sopose to obtain the highest maximum gain.

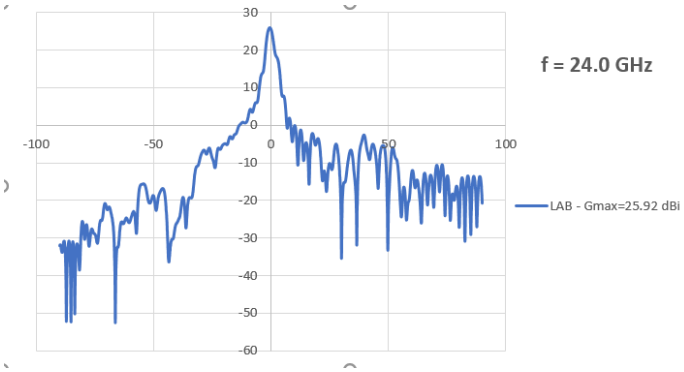

Fig. 21: Radiation pattern calculated from the experimental results at 24 GHz, with maximum gain information)

The resulting radiation pattern has a well defined maximum at zero degrees, with an obtained maximum gain of 25.92 dBi, a good result regarding the one obtained for the same frequency for the 10 cm RA

C. Reflection Results of the whole system

For the remaining experimental tests the goal is to measure the total S21 of the system, to analyse the insertion losses. In a perfect scenario, the insertion loss of the whole system would be 0 dB, meaning 100% of efficiency between horns. This efficiency will never achieve such result due to all the losses it has throughout all system components. Those losses include reflection at the port 1 entry; horn antenna losses; spill-over from illuminating the 30 cm RA; larger RA radiation efficiency, due to phase errors; Gaussian beam non-perfect definition, spill-over from illuminating the 10 cm RA; smaller RA radiation efficiency and Rx horn insertion losses.

The S21 results are obtained for different depths (mm), meaning, for different distances between two components. For the studied distance, 1500 mm, three results, for three different frequencies, were obtained.

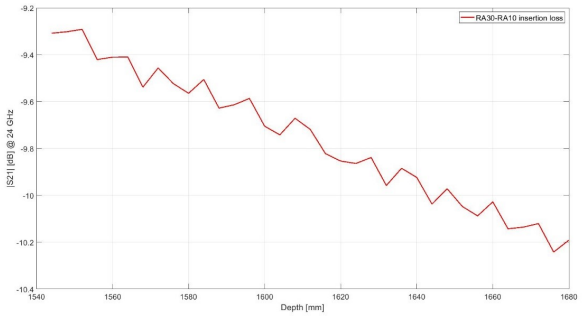

Fig. 22: insertion loss between the 30x30 cm RA and the 10x10 cm RA, S21 TOTAL, at 24 GHz)

The insertion losses obtained at 1500 mm, for 24 GHz, 24.5 GHz and 24.03 GHz respectively, were -8.924 dB, -9.648 dB and -8.87 dB. These results correspond also to efficiencies of 12.81% 10.84% and 12.97%Èventhough these

results represent an increased efficiency when compared with other state of the art, they also shows that the system may have its limitations for this type of context approach.

VIII. Conclusions and Future Work

A. Conclusions

The main idea of this dissertation is to study two different reflect arrays, with different sizes (1U and 3U) and their capability of radiating the beam to the position where the other CubeSat stands. This study performs by proposing two RAs, one of 10x10 cm, and the other of 30x30 cm, that are populated with unit cells to phase shift the circular reflected beam to the desired direction, now as a Gaussian Beam with a planar phase. The two lenses are simulated, after studying their behaviour on a program called KH3D, using the software CST-MWS. The 10x10 cm lens proved to be efficient in terms of performance, with a maximum gain at 25.09 and a total efficiency of 94.08% and a slight deviation of the main beam direction (1 degree). The 30x30 cm lens also proves to fulfil its goal, even though the best performance is deviated in the frequency, for ones higher than 24 GHz. After the creation and fabriation of the prototypes, it is time to proceed to the laboratorial exercises, where further simulations, now with both prototypes, are performed. The 10x10 cm lens performance proves, once gain, to be of high standard. The radiation pattern is similar to the obtained via CST and the obtained maximum gain is of 24.81, leading to a difference of 0.28 dBi from the CST. When comparing to the same results for other four and range close frequencies, not only the obtained gains are higher but the difference hits its lowest value. For the 30 cm RA, even though the results are satisfactory, with a well defined main lobe and a reasonable maximum gain, they cannot be compared to the CST simulations, since due to the file size it was not possible to obtain the maximum gain for it. With both lenses studied individually, the system could then be simulated to understand how the insertion loss, S21, was working through the depth. For two distinct depths, 1544 mm and 1600 mm, the the obtained insertion losses were -9.31 dB and -9.705, respectively, leading to an efficiency of 11.74% and 10.70%.These results prove to be an improvement, when compared to other solutions presented in previous studies. However, from an usability point of view, it still has its limitations for satellites use purposes.

B. Future Work

The 10x10 cm RA lens, despite eventual human errors, proves to perform the needed and desired behaviour to successfully wireless power transfer on a small distance of 1.5 m. On the CST simulation results, the lens deviated the beam in one degree. It would be important to understand the impact of unit cells' design errors on the aperture's performance. As mentioned before, the 30x30 cm RA was troublesome, due to its extremely large file size. The resultant CST radiation pattern was "broken". Furthermore, it was deviated in the frequency, meaning its best result could not be used for the desired frequency.

Another way of trying to improve the efficiency results would be to increase the reflectarrays area, to decrease the losses by spill-over. This reduces the aperture efficiency, so a middle term should be achieved.

In sum, the main subject of improvements is the reduction of energy losses by spill over.

References

[1] M. N. Sweeting, ""Modern Small Satellites - Changing the Economics of Space",," Proceedings of the IEEE, vol. 106, no. 3, 2018. .

[2] S. W. Janson, "25 Years of Small Satellites," SSC11-III-1

[3] A. H. Abdelrahman, A. Z. Elsherbeni and F. Yang, "Transmission Phase Limit of Multilayer Frequency-Selective Surfaces for Transmitarray Designs," IEEE Transactions on Antennas and Propagation, vol. 62, Februrary 2014.

[4] "Phased Array," [Online]. Available: https://en.wikipedia.org/wiki/Phased_array. [Accessed 03 june 2020].

[5] N. Parinaz, S. A. Matos, J. R. Costa and C. A. Fernandes, "Phase-Delay Versus Phase-Rotation Cells for Circular Polarization Transmit Arrays - Application to Satellite Ka-Band Beam Steering," Antennas and Propagation, vol. 66, no. 3, pp. 1236-1247, 2018.

[6] E. B. Lima, S. A. Matos, J. R. Costa, C. A. Fernandes and N. J. G. Fonseca, "Circular Polarization Wide-Angle Beam Steering at Ka-Band by In-Plane Translation of a Plate Lens Antenna," Antennas and Propagation, vol. 63, no. 12, pp. 5443-5455, december 2015.

[7] "Guide to the Nuclear Wall Chart," [Online]. Available: https://www2.lbl.gov/abc/wallchart/chapters/13/10.html. [Accessed 12 July 2020]. [Accessed 12 july 2020].

[8] S. Sasaki and K. Tanaka, "Wireless Power Transmission Technologies for Solar Power Satellite," in 2011 IEEE MTT-S International Microwave Workshop Series on Innovative Wireless Power Transmission: Technologies, Systems, and Applications, Kyoto, Japan, 2011.

[9] C. Bergsrud and J. Straub, "A space-to-space microwave wireless power transmission experiential mission using small satellites," pp. 193-203, 02 july 2014.

[10] D. R. Smith, V. R. Gowda, O. Yurduseven, S. Larouche, G. Lipworth, Y. Urzhumov and M. S. Reynolds, "An Analysis of Beamed Wireless Power Transfer in the Fresnel Zone using a Dynamic, Metasurface Aperture," Journal of Applied Physics, 2017.

[11] A. Z. Elsherbeni, P. Nayeri and F. Yang, "Reflectarray Antennas for Space Applications," in IEEE International Conference on Ultra-Wideband, Syracuse, NY, USA, 2012.

[12] "RP - photonics," [Online]. Available: https://www.rp-photonics.com/gaussian_beams.html. [Accessed 13 august 2020].

[13] C. A. Balanis, Antenna theory analysis and design, third ed., New Jersey: John Wiley Sons, Inc, 2005.

[14] R. Pereira e N. Carvalho, Quasioptics for Increasing the Beam Efficiency of Wireless Power Transfer Systems, Research Square, Wireless Power Week, 2022.